J Comp Physiol A (1998) 183: 225–235

ORIGINAL PAPER

J. P. Danaceau · M. T. Lucero

Betaine activates a hyperpolarizing chloride conductance in squid olfactory receptor neurons

Accepted: 20 March 1998

Abstract Isolated olfactory receptor neurons from the squid *Lolliguncula brevis* respond to betaine, a repellent odorant, with hyperpolarizing receptor potentials. Using perforated-patch techniques, we determined that the hyperpolarizing conductance was selective for Cl^- and could be reversibly blocked by the Cl^- channel blockers 4-acetamido-4′-isothio-cyanatistilbene-2,2′disulfonic acid and niflumic acid. Gramicidin-patch recordings revealed that $[Cl^-]_i$ in squid olfactory receptor neurons is normally very low compared to vertebrate olfactory receptor neurons, and that activating a Cl^- conductance would hyperpolarize the cell in vivo. The lack of dependence on internal or external K^+ or Na^+ ruled out the possibility that the Cl^- conductance was generated by a cation-dependent cotransporter or pump. Common G-protein-dependent signalling pathways, including phospholipase C, arachidonic acid, and cyclic nucleotides, do not appear to be involved. Ca^{2+} imaging experiments showed that betaine did not affect $[Ca^{2+}]_i$, suggesting that the Cl^- current is not Ca^{2+} dependent. Our findings represent the first report of an odorant-activated, hyperpolarizing chloride conductance in olfactory receptor neurons.

Key words Betaine · Chloride · Gramicidin Perforated patch · Cephalopods

Abbreviations *ASW* artificial seawater · *cAMP* cyclic adenosine-5′-monophosphate · C_M cell capacitance · *CNG channel* cyclic nucleotide gated channel · *DMSO* dimethylsulfoxide · E_{Cl} chloride reversal potential · E_{rev} reversal potential *Gluc*$^-$ D-gluconic acid · *Glut*$^-$ L-glutamic acid · *GP* gramicidin patch · IP_3 inositol 1,4,5 triphosphate · *I-V* current-voltage relationship · *ORNs* olfactory receptor neurons · R_M membrane input resistance · R_S series resistance · *SITS* 4-acetamido-4′-isothio-cyanatistilbene-2,2′disulfonic acid · TMA^+-tetramethyl-ammonium · *WC* whole cell

J. P. Danaceau · M. T. Lucero (✉)
Department of Physiology,
University of Utah,
School of Medicine,
Salt Lake City, UT 84108, USA
e-mail: Mary.Lucero@m.cc.utah.edu
Tel.: +1-801-5855601; Fax: +1-801-5813476

Introduction

Binding of an odorant to a G-protein coupled receptor (Buck and Axel 1991) generates second messengers within the cilia of olfactory receptor neurons (ORNs). The link between odor stimulation, activation of cyclic-nucleotide-gated (CNG) channels by cAMP, and depolarization of vertebrate ORNs is well established (Gold and Nakamura 1987; Firestein et al. 1991; Zufall et al. 1994). Debate continues on the role of alternative transduction mechanisms in vertebrates, although the involvement of phosphoinositides such as inositol 1,4,5-trisphosphate (IP_3) has been found in catfish (Bruch and Teeter 1989; Miyamoto et al. 1992; Restrepo et al. 1993), salmon (Lo et al. 1993) and rat (Boekhoff et al. 1990b; Breer et al. 1990; Ronnett et al. 1993). Among invertebrates, the evidence for a diversity of transduction pathways is more clear cut, and both the IP_3 and cAMP pathways have been identified in several organisms including lobster (Fadool and Ache 1992), squid (Lucero and Piper 1994), cockroach (Breer et al. 1990; Boekhoff et al. 1990a) and moth (Stengl et al. 1992).

One function proposed for multiple second-messenger pathways in ORNs is transduction of depolarizing and hyperpolarizing responses (Dionne and Dubin 1994; Ache and Zhainazarov 1995). Hyperpolarizing responses of vertebrate ORNs to odors have been reported in frog (Gesteland et al. 1965), toad (Morales et al. 1994) and catfish (Kang and Caprio 1995). Hyperpolarizing responses of invertebrate ORNs to odors have been reported in squid and moth (Stengl et al. 1992; Lucero and Piper 1994) and have been well characterized in lobster (McClintock and Ache 1989; Michel and Ache 1992). Although a number of mechanisms may underlie

hyperpolarizing responses, activation of ionic conductances with negative reversal potentials (K^+, Cl^-) are the most common.

Recently, odorant-induced increases in Cl^- conductance have been reported in turtle (Kashiwayanagi et al. 1996), amphibians (Kleene and Gesteland 1991; Kleene 1993; Kurahashi and Yau 1993; Firestein and Shepherd 1995; Delay et al. 1997) and mammals (Lowe and Gold 1993; Restrepo et al. 1996). However, unlike most types of neurons, where $[Cl^-]_i$ is low and activation of a Cl^- conductance hyperpolarizes the cell, in vertebrate olfactory receptor neurons, $[Cl^-]_i$ is estimated to be relatively high. In *Xenopus* ORNs, the normal $[Cl^-]_i$ is 119 mmol·l^{-1} and the Cl^- reversal potential (E_{Cl}) is approximately 0 mV (Zhainazarov and Ache 1995); opening a Cl^- channel at negative potentials would drive Cl^- efflux and depolarize the cell. In mudpuppy, E_{Cl} is estimated at −45 mV which could either potentiate a depolarization or, if Cl^- channels close, could hyperpolarize ORNs (Dubin and Dionne 1994). To date, the only report of an increased Cl^- conductance in ORNs, that may mediate a hyperpolarizing response, has been a preliminary account of our own work on squid ORNs in abstract form (Lucero and Piper 1994). In this study, we have used betaine, a behaviorally aversive odorant to squid, cuttlefish, nautilus (Lee et al. 1994), and octopus (Lee 1992), to investigate the hyperpolarizing chloride conductance in ORNs from the squid, *Lolliguncula brevis*.

Materials and methods

Cell preparation and culture conditions

The methods for cell dissociation were similar to those described in Lucero et al. (1992). Briefly, the olfactory organs of the squid *L. brevis*, were excised under a dissecting microscope and treated with non-specific protease (10 mg ml^{-1}; Sigma type XIV) in sterile filtered artificial seawater (ASW) for 50 min. Following a 3- to 5-min rinse in sterile filtered ASW, the olfactory organ was plated onto a drop of culture medium on concanavalin A (10 mg ml^{-1}; Sigma type IV)-coated glass coverslips and allowed to settle for 15 min before adding 2 ml culture medium and placing in the incubator at 22 °C. Culture media was changed daily and cells were used for experiments between 1 and 3 days in culture. Only the pyriform receptor cell type was used in these experiments (Lucero et al. 1992).

Solutions

The external bath solutions and internal pipette solutions are listed in Tables 1 and 2, respectively. The osmolality of 780 mosmol kg^{-1} was chosen because it is in the midrange of osmolalities of the seawater that this species of squid inhabits. The betaine bath solutions were made fresh daily and the pH was set to pH 7.4. Culture medium consisted of Leibovitz's L-15 (Gibco, Grand Island, N.Y.) supplemented with salts to bring the osmolality to 780 mosmol kg^{-1}, 2 mmol·l^{-1} Hepes, 4 mmol·l^{-1} L-glutamine, 200 units ml^{-1} penicillin G and 200 mg ml^{-1} streptomycin sulfate (Irvine Scientific, Santa Ana, Calif.). The media was set to pH 7.6 using NaOH and immediately sterile filtered. All chemicals were obtained from Sigma Chemical, St. Louis, Mo. unless stated otherwise.

Blockers

Two chloride channel blockers were used: 4-acetamido-4′-isothiocyanatistilbene-2,2′disulfonic acid (SITS), and niflumic acid. SITS was dissolved in ASW to 500 μmol·l^{-1}. A 20-mmol·l^{-1} stock solution of niflumic acid, made by sonication in dimethylsulfoxide (DMSO) was diluted to 100 μmol·l^{-1} in ASW. Control application of vehicle had no effect. Neomycin (100 μmol·l^{-1} and 1 mmol·l^{-1}) was dissolved in ASW. Stock solutions (4.3 mmol·l^{-1}) for the PLC inhibitor U-71322 and its inactive enantiomer, U-73343, were dissolved in DMSO and diluted to final concentrations in ASW.

Nystatin and gramicidin voltage- and current-clamp recordings

We used the nystatin perforated-patch recording technique to minimize perturbation of the cytosolic environment (Horn and Marty 1988). Nystatin forms non-selective monovalent ion chan-

Table 1 Composition of external bath solutions. All solutions were set to pH 7.4 with NaOH or tetramethylammonium hydroxide (TMAOH) and set to an osmolality of 780 mosmol kg^{-1} using D-glucose. EGTA 10 (mmol · l^{-1}) was added to the 0 Ca^{2+}-ASW. All concentrations are in millimoles per liter

Bath Solution	Na^+	K^+	Ca^{2+}	Mg^{2+}	Cl^-	$Tris^+$	Hepes	Glucose
ASW	340	10	10	35	440	0	10	17.5
0 Ca^{2+}-ASW	340	10	0	45	440	0	10	7.5
$TRIS^+$-SW	0	0	10	35	430	340	10	20

Table 2 Composition of internal pipette solutions. All solutions were set to pH 7.2 with TMAOH and were set to an osmolality of 780 mosmol kg^{-1} using D-glucose. Concentrations are in millimoles per liter. Pipette solutions also contained 10 mmol · l^{-1} Hepes and 1.5 m EGTA. (Abbreviations: *Glut* L-glutamic acid, $Gluc^-$ D-gluconic acid). Gramicidin and nystatin were added to the various internal solutions as described in Materials and methods

Pipette Solution	Na^+	K^+	Ca^{2+}	Cl^-	F^-	$Glut^-$	$Gluc^-$	TMA^+
TMA-Cl	25	0	0.5	366	25	0	0	365
KCl	0	430	0.5	406	25	0	0	0
KGlut	0	390	0.5	21	25	345	0	0
TMA-Glut	25	0	0.5	51	25	255	0	305
Na-Gluc	280	0	0.5	61	25	0	255	60

nels that allow electrical access to the cell, enabling manipulation of intracellular ions without dialyzing soluble second messengers associated with olfactory responses. A nystatin stock solution consisted of 1 mg per 20 µl DMSO. Three microliters of stock solution and 3 µl of 25% pluronic acid (used as a dispersal agent) were added to 1 ml of internal solution. Fresh nystatin interal solution was made every 2 h and the nystatin stock solution was remade every 5 h. Gramicidin was used to record from ORNs without perturbing $[Cl^-]_i$ (Myers and Hayden 1972). Gramicidin perforated-patch recordings were made according to the technique of Abe et al. (1994). The gramicidin stock solution consisted of 1 mg gramicidin per 100 µl methanol; 10 µl of this stock solution was added to 1 ml internal solution. All internal solutions were kept in the dark and on ice.

Electrodes (2–5 MΩ resistance in ASW) were pulled on a Flaming/Brown P87 puller from thick-walled borosilicate filament glass (Sutter Instrument, San Rafael, Calif.). Data from gramicidin-patch voltage-clamp recordings were obtained after series resistances (R_S) had dropped below 100 MΩ, approximately 15–30 min after gigaohm-seal formation. Whole cell recordings were made immediately following patch rupture. Bath solutions (21–23 °C) were perfused through the recording chamber at a rate of 1–2 ml min^{-1}. Test solutions were delivered either with a picospritzer connected to single- or multibarrel pipettes, or an SF-77 rapid solution changer (Warner Instrument, Hamden, Conn.). Initially, a silver-silver chloride pellet bath electrode was used to ground the bath solutions. In later experiments, a KCl-agar bridge was used. Because we never varied external Cl^- there was no difference in data from the two bath grounds.

Current-clamp recordings were made in the perforated-patch configuration. Immediately after electrical access was established, the clamp amplifier was switched from voltage clamp to current clamp under zero applied current. In some cells, a small current was injected to depolarize the cell slightly above threshold to record a steady train of action potentials (see Fig. 1B).

Data acquisition

Voltage-clamp and current-clamp recordings were made and digitized with a 125-kHz DMA Labmaster/TL-1-125 Interface (Axon instruments, Foster City, Calif.) and a 486, 33-MHz computer. Membrane voltages and currents were measured using an Axon Instruments 200A patch-clamp amplifier. Data acquisition rates ranged from 0.5 kHz to 50 kHz. Data were filtered at either 10 kHz or 1 kHz. Linear leak and voltage-gated currents were subtracted off line from all voltage-clamp data. Data analysis was performed using Chanal software (Biodiversity, Park City, Utah). The −2 to 18-mV liquid junction potentials between the various internal and external solutions were calculated using Axoscope (Axon Instruments) and corrected for off-line. A standard leak pulse protocol that consisted of averaging the currents (I) from 24 repeated 40-ms voltage (V) pulses that stepped from −70 mV to −80 mV was used to calculate membrane input resistance (R_M), by dividing ΔV by ΔI according to Ohm's law. Cell capacitances (C_M) were determined by integrating the area under the capacity transient to obtain the amount of charge moved (Q), and dividing Q by ΔV. Cells were voltage clamped to a given voltage for 800–1000 ms to allow time for voltage-gated currents to stabilize before odorant application. The average uncompensated R_S associated with access between the pipette, the perforated patch, the soma and the ciliary region was 45 ± 8 MΩ (SD; n = 11); 70–80% of R_S was electrically compensated on-line. Voltage errors associated with the residual uncompensated R_S were corrected off-line according to Ohms's law: $V = V_P - (I_{total})(R_S)$, where V = cell potential, V_P = pipette or command potential, and I_{total} = peak current plus leak current during a betaine response (Marty and Neher 1995). All values are presented as the mean ± standard deviation (SD); n = number of cells.

Intracellular calcium measurements

Ca^{+2}-imaging experiments were carried out on ORNs dissociated and plated as described above. Cells were loaded with 5 µmol·l^{-1} Fura-2/AM (Grynkiewicz et al. 1985) plus pluronic F127 (80 µg ml^{-1}) in filtered ASW at 23 °C in the dark for 20 min (followed by four washes in ASW). Changes in intracellular $[Ca^{+2}]$ were measured from the background-corrected ratio of fluorescence at 340/380 nm. A Zeiss–Attofluor imaging system and software (Atto Instruments, Rockville, Md.) was used to acquire and analyze the data. Data points were sampled at 1 Hz. Betaine was delivered by bath exchange using a large volume loop injector (1–2 ml). Positive controls included 10 mmol·l^{-1} caffeine, 10 mmol·l^{-1} dopamine, and 50 mmol·l^{-1} KCl made up in ASW.

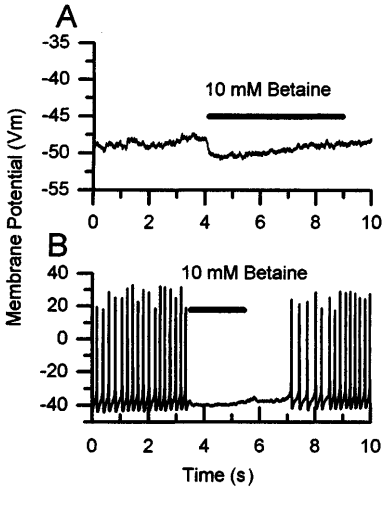

Fig. 1A, B Betaine hyperpolarizes squid olfactory receptor neurons (ORNs) and inhibits the firing of action potentials. **A** Application of 10 mmol·l^{-1} betaine to a nystatin-patched, current-clamped squid ORN hyperpolarized the cell from rest. **B** Betaine application inhibited the action potentials elicited by injecting a small, depolarizing current. Solutions: K-Glut int./artificial seawater (ASW) ext.

Results

Perforated-patch recordings of squid ORNs have higher membrane input resistances than whole-cell recordings

Whole-cell recordings of the passive properties of ORNs from the squid *L. brevis* have shown that the mean R_M is 145 ± 8 MΩ (n = 30) (Lucero and Chen 1997). In the present study, using either nystatin or gramicidin for perforated-patch recordings, the R_M (measured as described in Materials and methods) was nine times higher and averaged 1288 ± 1645 MΩ (n = 11). Initial seal resistances of 5–10 GΩ were the same for both recording conditions. The large decrease in the input resistance observed during whole-cell recording suggests that whole-cell dialysis of second-messenger systems and Ca^{2+} buffering increases the activity of leak channels in the membrane. In perforated-patch recordings, the total capacitance measured by integration was 53.5 ± 30.8 pF (n = 11). This capacitance was similar to ciliary whole-cell capacitances that averaged 63.3 ± 27.5 pF (n = 26) (Lucero and Chen 1997).

Betaine hyperpolarizes squid ORNs by activating a chloride-selective conductance

In the squid *L. brevis*, application of betaine hyperpolarizes ORNs. In Fig. 1, nystatin-patched current-clamp recordings made from an isolated *Lolliguncula* ORN, show that betaine hyperpolarizes the cell and inhibits the firing of action potentials. Of the 741 cells tested with betaine alone, 460 (62%) responded.

Because of the difficulty of teasing out multiple conductances in current clamp, voltage-clamp recordings were made to determine the ionic selectivity of the betaine responses. In all of the following figures, the first 500 ms containing transient voltage-gated currents have been omitted. The steady-state voltage-dependent and linear leak currents have been baseline subtracted so that only the odor-sensitive currents are shown. To test the dependence of the betaine responses on Na^+ and K^+, we replaced internal K^+ with tetramethylammonium (TMA^+), and replaced external NaCl and KCl with TRISCl. Figures 2A and B show betaine responses in nystatin-patched ORNs in the presence and absence of external Na^+ and K^+. The shapes of the betaine-activated currents were very similar. Current-voltage (I-V) relationships obtained by plotting the peak current for betaine responses in the presence and absence of external Na^+ and K^+ are shown in Fig. 2C and D. The reversal potentials (E_{rev}) for betaine responses in normal ASW and TMA-Cl internal solution averaged -4 ± 4 mV ($n = 12$) and were not significantly different from the E_{rev} of -6 ± 10 mV ($n = 11$) when external Na^+ and K^+ were completely replaced by $TRIS^+$ (Student's *t*-test, $P > 0.1$). The slopes of the averaged I-V relationships were also not significantly different (2.2 ± 1.6) in ASW compared to 1.9 ± 1.2 in TRIS-ASW ($P > 0.1$).

There was no effect on betaine-activated conductances, and minimal reduction in current amplitudes, when Na^+ and K^+ were eliminated from internal and external solutions. However, when we altered E_{Cl}, the reversal potentials of responses to betaine shifted as would be predicted by the Nernst equation for a Cl^--selective conductance. Because the cells became too fragile to record from when external Cl^- was reduced, we varied the $[Cl^-]_i$ of the nystatin internal solutions. In Fig. 3A, only outward currents were recorded at voltages positive to -50 mV from a nystatin-patched voltage-clamped ORN that had a calculated E_{Cl} of -50 mV. In a different cell, where E_{Cl} was set to -5 mV by changing $[Cl]_i$, the E_{rev} of the betaine response shifted to -5 mV (Fig. 3B). In Fig. 3C, plots of current-voltage (I-V) relationships for the betaine-induced currents from Figs. 3A and 3B show that the E_{rev} of the betaine response follows E_{Cl}. In Fig. 3D we have plotted the averaged E_{rev} of the responses to 10 mmol $\cdot 1^{-1}$ betaine

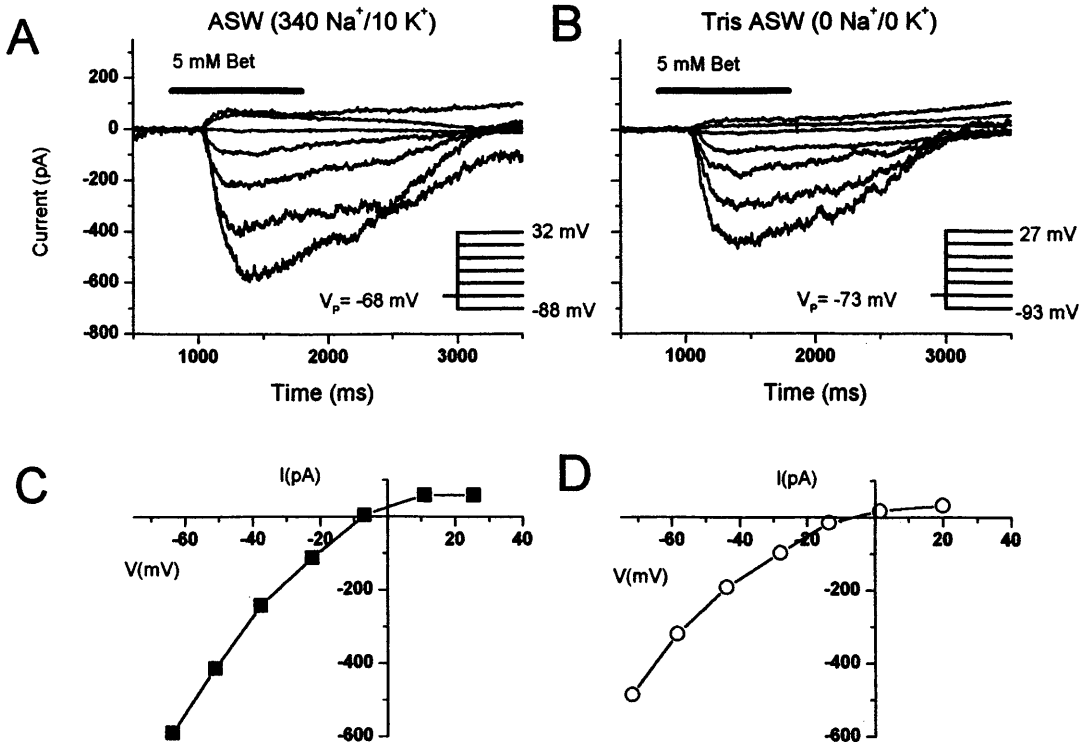

Fig. 2A–D Betaine-activated currents are not dependent on external Na^+ or K^+. Betaine-activated currents from a nystatin-patched squid ORN are shown in the presence **A** and absence **B** of external Na^+ and K^+. Command voltages (V_P) corrected for junction potentials are shown on the protocols. **C** and **D** Current-voltage (I-V) relationships for the peak currents elicited in **A** and **B** have been corrected off-line for series resistance as described in Materials and methods, and show that in $TRIS^+$, betaine responses are only slightly reduced and have the same reversal potential as in ASW. Solutions: TMA-Cl int./ASW ext. and TMA-Cl int./TRIS-ASW ext.

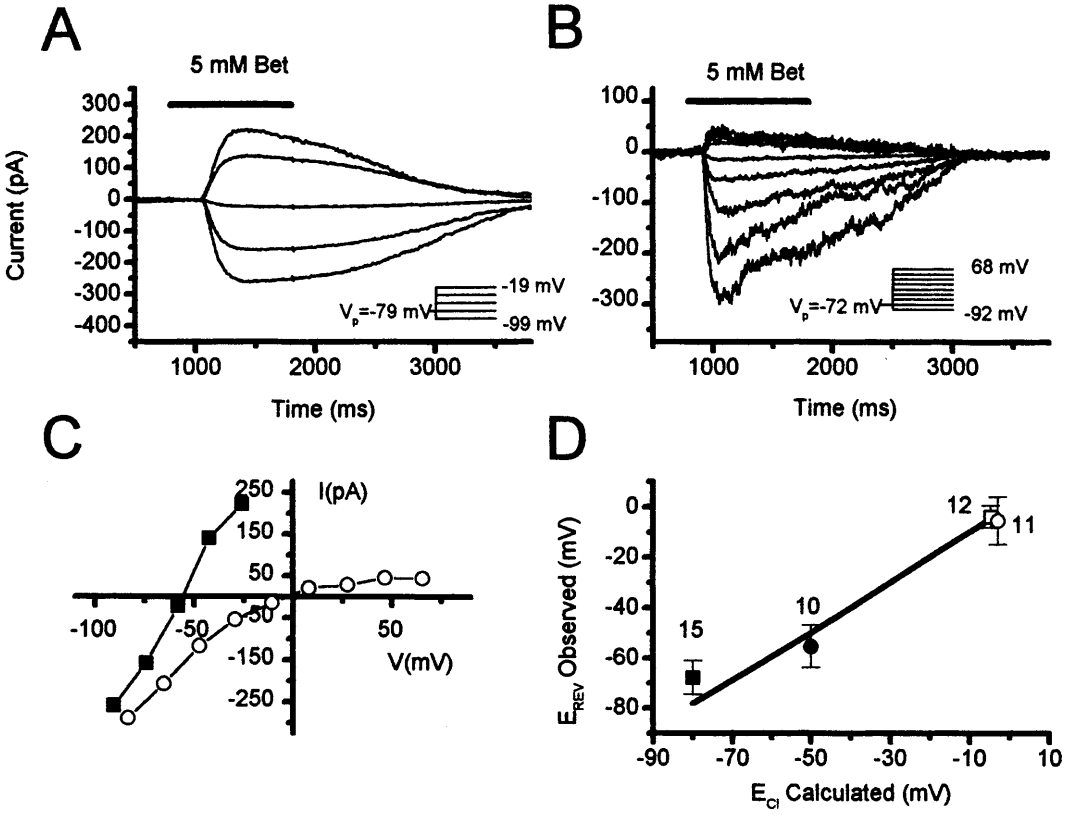

Fig. 3A–D The betaine-induced current is carried by Cl^-. **A** When the Cl^- reversal potential (E_{Cl}) was set to −50 mV, applying command voltages (V_P) from −99 to −19 mV for 4 s while delivering a 1-s spritz of 10 mmol · l^{-1} betaine resulted in currents that reversed at −56 mV. Solutions: Na-Gluc int./ASW ext. **B** In a different nystatin-patched cell, E_{Cl} was set to −5 mV and applying 5 mmol · l^{-1} betaine for 1 s (*solid bar*) during 4-s command voltage steps (V_P) from −92 mV to +68 mV resulted in currents that reversed at −5 mV. Solutions: TMA-Cl int./ASW ext. **C** I-V relationships are plotted for the traces in **A** (*solid squares*) and **B** (*open circles*) above and have been corrected for series resistance (R_s). **D** A plot of observed reversal potential (E_{rev}) versus calculated E_{Cl} shows that the betaine-induced currents followed the Nernst potential for Cl^- when Cl^- or gluconate were the internal anions (*open square*, *open circle* and *solid circle*) but deviated slightly when glutamate was the internal anion (*solid square*). All Cl^- concentrations were corrected using Cl^- activity coefficients (Robinson and Stokes 1968) before using the Nernst equation to calculate E_{rev}. *Error bars* indicate ± SD. *Numbers* indicate numbers of cells. Solutions: *solid square* K-Glut int./ASW ext.; *solid circle* Na-Gluc int./ASW; *open square* TMA-Cl int./ASW; *open circle* TMA-Cl int./TRIS-ASW

versus the calculated E_{Cl}. When TMACl and $TRIS^+$-ASW solutions were used, the calculated (−3 mV) and observed E_{rev} (−6 ± 10 mV, $n = 11$) were the same (open circle). When a low Cl^- internal solution was used, the calculated E_{Cl} was more negative than the observed E_{rev} (−78 and −68 ± 7 mV, $n = 15$, respectively; solid square). Further studies showed that the deviation from E_{Cl} at negative potentials was due to a slight permeability of the Cl^- channels to glutamate, the major anion in the low Cl^- internal solution. When gluconate was used as the internal anion (solid circle), the betaine responses closely followed the predicted values (indicated by the solid line) for a Cl^- selective conductance. The relative permeability of glutamate to Cl^- (Pglutamate/PCl^-) of 0.03 was calculated using the Goldman, Hodgkin, and Katz voltage equation (Hille 1992), and is similar to the relative glutamate permeability in frog muscle of 0.02 (Woodbury and Miles 1973).

E_{Cl} is negative in squid ORNs

Our nystatin-patch recording configurations perturbed $[Cl]_i$. Consequently, betaine application would hyperpolarize or depolarize cells depending on where we set E_{Cl}. In order to understand the physiological consequences of odorants that activate a Cl^- conductance in squid ORNs, we had to determine the resting E_{Cl}. With an E_{Cl} negative to rest, betaine stimulation would hyperpolarize the cell and reduce any tonic activity. Stimulating a cell with a more positive E_{Cl} should result in a depolarization and increase tonic activity. To measure the resting E_{Cl}, we included the antibiotic gramicidin with a high KCl internal solution in the patch pipette. Unlike nystatin, gramicidin pores are impermeable to Cl^- ions, and so recordings can be made with minimal disturbance of the normal $[Cl]_i$ of the cell (Myers and Hayden 1972; Abe et al. 1994; Zhainazarov and Ache 1995). Figure 4A shows a family of betaine-activated currents from a gramicidin-patched (GP) cell. Betaine activated inward currents at pipette voltages (V_P) negative to −68 mV and outward currents at V_P positive to −68 mV. In Fig. 4B, recorded from the same

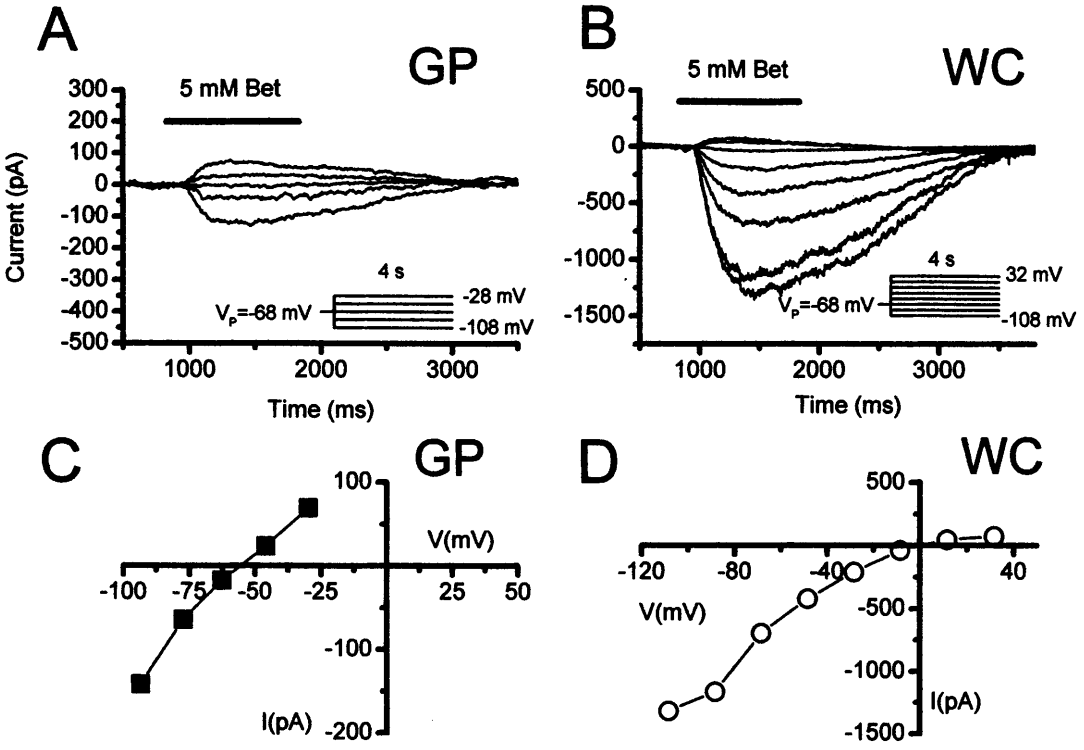

Fig. 4A–D Squid ORNs have a low $[Cl^-]_i$. **A** Three minutes after achieving stable R_s, a 1-s application of 5 mmol l^{-1} betaine to a gramicidin-patched (GP) squid ORN during each 4-s command voltage step (V_P) from −108 to −28 mV resulted in currents that reversed at negative potentials. Solutions: TMA Cl int./ASW ext. In the same cell, E_{rev} shifted towards 0 mV 2 min after rupturing the patch and attaining whole-cell (WC) access. **C** and **D** I-V plots were made from the peak currents shown in **A** (*solid squares*) and **B** (*open circles*) above. The calculated E_{Cl} based on the pipette solution was −5 mV, and was 52 mV positive to the reversal potential measured before internal Cl^- was perturbed. The slight discrepancy between the voltages of the I-V in **C** and **D** and the voltage protocols in **A** and **B** is from R_S correction as described in Materials and methods

cell, we applied suction to rupture the membrane patch and replaced the normal $[Cl^-]_i$ with that of the patch pipette (406 mmol $\cdot$ l^{-1} Cl^-). In whole-cell (WC) mode, inward current responses were observed at voltages that in GP mode only showed outward currents. The I-V relationships made from the peak currents in Figs. 4A and 4B and corrected for R_s as described in Materials and methods, are plotted in Figs. 4C and 4D, respectively. In this cell, E_{rev} shifted from −57 mV to −4 mV and the slope conductance increased from 2.6 nS to 4.2 nS after rupturing the membrane patch. Experiments using nystatin (Cl^- permeant) had similar R_S yet E_{rev} did not shift upon patch rupture, indicating that the shift observed using gramicidin is due to a change in $[Cl^-]_i$ rather than a decrease in R_S.

One concern we had was that as series resistance decreased, chloride may leak into the cell through the patch and perturb $[Cl]_i$ during the recording. Figure 5 shows a plot of the measured E_{rev} and R_S versus time for the cell shown in Fig. 4. As R_S decreased, the E_{rev} of the betaine response actually became more negative, the

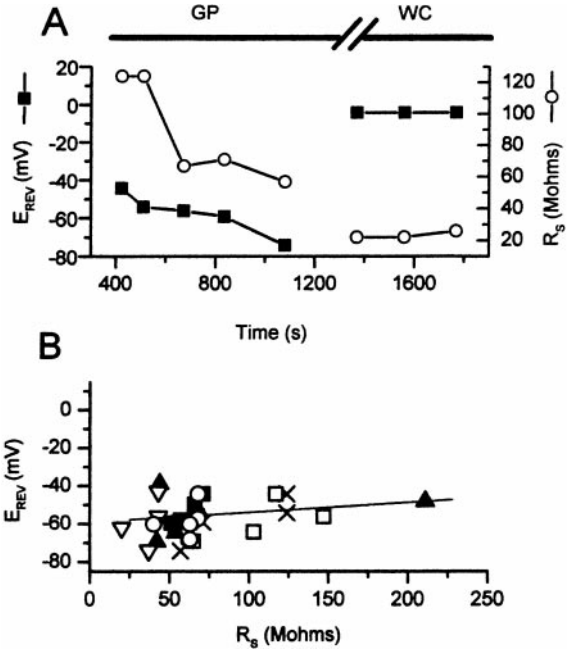

Fig. 5A, B E_{REV} of betaine responses in GP are stable relative to changes in time or R_s. **A** Plot of E_{rev} (*black squares*) and series resistance (*open circles*) versus time for the cell shown in Fig. 4 during GP and WC configurations. **B** Plot of E_{rev} versus R_S in the cells used in the GP experiments. A linear regression fit to the data resulted in values of 0.29, 0.08, and 0.12, the correlation coefficient (r), slope of the line (m), and probability of association (p), respectively. Each symbol (*filled triangles*, *filled circles*, *filled squares*, *crosses*, *open squares*, *open inverted triangles*, and *open circles*) represents data obtained from a different cell

opposite of what would be expected if the high $[Cl^-]_i$ of the patch pipette was leaking through the gramicidin patch. Figure 5A also shows that after the R_S of the gramicidin patch had stabilized, the E_{rev} of betaine responses continued to shift slightly more negative suggesting that as R_S decreased, the accuracy of our measure of the natural E_{Cl} increased. When WC access was obtained, there was an immediate shift in E_{rev} from −74 mV (the cell's natural E_{Cl}) to −4 mV (the E_{Cl} of these solutions) and a decrease in R_S from 57 MΩ to 22 MΩ. Figure 5B shows a plot of R_S versus E_{rev} for all seven cells used in the gramicidin patch experiments. A line fit to the data shows that there is no significant relationship between R_S and E_{rev}, indicating that changes in series resistance do not account for the difference in E_{rev} in gramicidin-patch versus WC modes.

In gramicidin-patch recordings using KCl internal and ASW, the average E_{rev} of the betaine response was −57 ± 5 mV ($n = 7$). This corresponds to a $[Cl^-]_i$ of ~50 mmol·l^{-1}. After WC access was obtained, the E_{rev} shifted to 1 ± 13 mV ($n = 19$). The difference between the E_{rev} of betaine responses obtained in WC and gramicidin-patch configurations was statistically significant (Student's t-test; $P < 0.01$). The slope conductances of the responses also increased significantly (Student's t-test; $P < 0.05$) from an average value of 1.9 ± 1.0 nS to 4.7 ± 3.9 nS ($n = 7$ and 19, respectively). We attribute the conductance increase to both a decrease in R_S associated with WC mode, and the greater driving force on Cl^- at negative potentials when E_{Cl} is near 0 mV. These experiments provide clear evidence that the natural E_{Cl} of squid ORNs is more negative than has been reported in ORNs from other species, and that betaine would tend to hyperpolarize tonically firing cells in vivo.

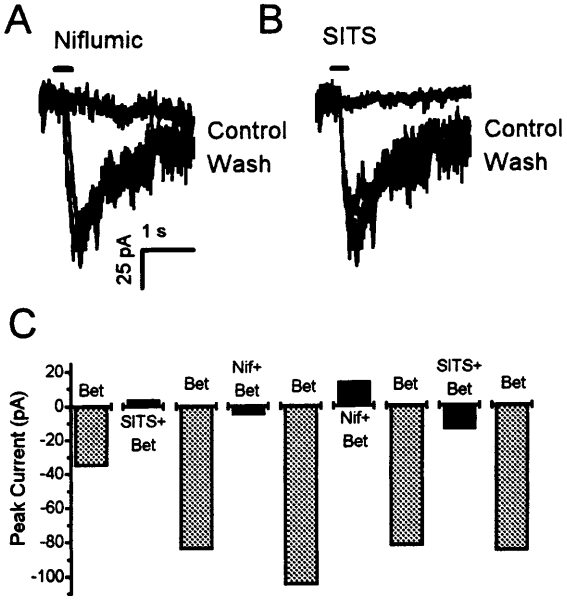

Fig. 6A–C Cl^- channel blockers reversibly inhibit betaine-induced currents. **A** Superimposed current traces were obtained during sequential 300-ms applications of 5 mmol·l^{-1} betaine (*Control*), 5 mmol·l^{-1} betaine + 100 μmol·l^{-1} niflumic acid, and 5 mmol·l^{-1} betaine (*Wash*). The test voltage was −52 mV. Solutions: TMA-Cl int./ASW ext. **B** Superimposed current traces from the same cell as **A** with sequential application of 5 mmol·l^{-1} betaine (*Control*), 5 mmol·l^{-1} betaine + 500 μmol·l^{-1} SITS, and 5 mmol·l^{-1} betaine (*Wash*). **C** Reversible block by 500 μmol·l^{-1} SITS and 100 μmol·l^{-1} niflumic acid of the betaine-induced current in the same nystatin-patched cell. *Bars* indicate absolute peak current values during sequential 300-ms applications of indicated substances. Small inward and outward currents observed with sequential application of each blocker were within the noise of the recording

Pharmacology of odorant-induced chloride currents

We used the Cl^- channel blockers niflumic acid and SITS to pharmacologically characterize the odorant-induced Cl^--selective conductance. Figures 6A and B show that at −52 mV, 100 μmol·l^{-1} niflumic acid and 500 μmol·l^{-1} SITS reversibly block the responses to 5 mmol l^{-1} betaine. In Fig. 6C, we plot the peak current during sequential applications of betaine and betaine plus the channel blockers. The small residual outward current observed in the presence of betaine plus SITS was within the noise (< 5 pA) of the recording and was measured as a small inward current in the subsequent application of niflumic acid. The gradual increase in the size of the betaine-induced current reflects the increased access through the nystatin patch. While both agents blocked betaine responses in all cells tested, recovery was not always complete. Five of seven cells tested showed complete recovery to 100 μmol·l^{-1} niflumic acid and five of eight cells showed complete recovery to 500 μmol·l^{-1} SITS. The block of betaine responses by two different Cl^- channel blockers supports our hypothesis that betaine activates a signal transduction cascade which results in the opening of Cl^- channels.

Squid ORNs respond to betaine in a dose dependent manner

Application of 10 mmol·l^{-1} betaine to different ORNs activated Cl^- currents that ranged from 15 pA to over 200 pA. The large cell-to-cell variability in the magnitude of the betaine responses could be due to differences in receptor and channel densities or due to variability in electrical access afforded by the perforated-patch technique. To minimize variability due to electrical access, concentration-response experiments were performed after the current amplitude responses to a single concentration of betaine had stabilized (~15 to 30 min). In addition, capacitance measurements were made before and after application of each betaine concentration and only cells with stable capacitance measurements were included. Finally, the concentration-response data for a given cell was normalized to the peak current elicited by 100 mmol·l^{-1} betaine in the same cell. The inset in Fig. 7 shows the currents from a single cell that was spritzed with 100 μmol·l^{-1}, 1 mmol·l^{-1} and

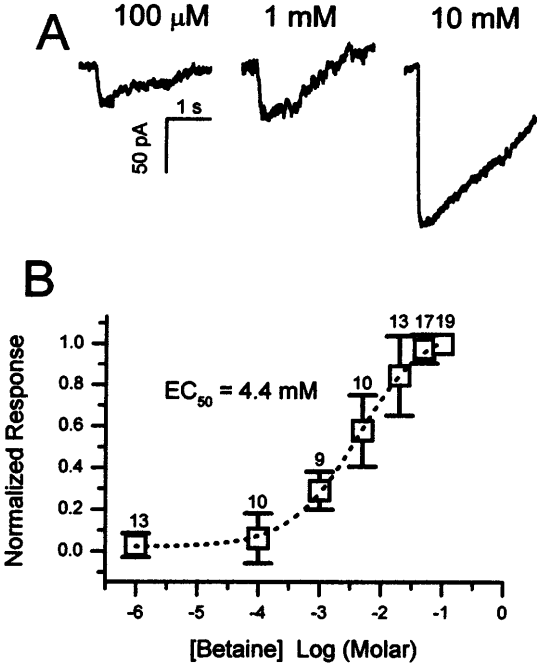

Fig. 7A, B Betaine-induced currents are dose dependent with an EC_{50} of 4.4 mmol · l^{-1} and a Hill coefficient of 0.9. **A** Nystatin-patched squid ORNs were held at −52 mV for 4 s while receiving a 0.3-s application of a given betaine concentration. Sequential applications of 100 μmol · l^{-1}, 1 mmol · l^{-1} and 10 mmol · l^{-1} betaine resulted in increasing current responses. Solutions: TMA-Cl int./ASW ext. **B** The averaged concentration-response curve for normalized peak betaine-induced currents at −52 mV plotted against the log of betaine concentration, was fitted with the Hill equation to obtain the EC_{50} and the Hill coefficient. *Error bars* indicate ± SD; *numbers of cells* are indicated above each data point

10 mmol · l^{-1} betaine. A Hill plot of the averaged data from 19 cells revealed an EC_{50} of 4.4 mmol · l^{-1} and a Hill coefficient of 0.9, suggesting that there is little cooperativity in this system and that it provides a broad concentration response range compared to odorants in other olfactory systems.

Betaine responses are not mimicked by common second messengers

Because our initial experiments using a different aversive odorant (dopamine) (Gilly and Lucero 1992) showed involvement of the phospholipase C/IP_3 pathway (Lucero and Piper 1994) and increases in $[Ca^{2+}]_i$ (Lucero et al. 1995), we investigated the role of these second messengers in the betaine response. In nystatin-patch experiments, we found that inhibitors of the IP_3 pathway including neomycin (100 μmol · l^{-1}, $n = 4$; 1 mmol · l^{-1}, $n = 3$) and U-71322 (5 μmol · l^{-1}, $n = 5$; 25 μmol · l^{-1}, $n = 10$) had no effect on betaine responses.

We also used Ca^{2+}-imaging techniques to determine if betaine elicited changes in intracellular Ca^{2+}. We found that betaine did not increase or decrease $[Ca^{2+}]_i$ ($n = 21$). Given that 60% of the cells respond electrically to betaine, we would have expected to see 13/21 cells respond if calcium was involved. To verify that the cells were competent, positive controls were run using dopamine, caffeine, and high K^+. All of these compounds increased $[Ca^{2+}]_i$ (data not shown).

Having ruled out the phospholipase C pathway and Ca^{2+}, we tested whether or not arachidonic acid could mimic the betaine response and activate a Cl^- current. We found that 10 μmol · l^{-1} arachidonic acid had no effect on nystatin-patched squid ORNs ($n = 7$). Finally, it is unlikely that the cAMP pathway is involved in activating the betaine-dependent Cl^- current, because inclusion of cAMP in the pipette depolarized squid ORNs and voltage responses did not follow E_{Cl} (Lucero and Piper 1994). Further experiments will determine if betaine directly activates the Cl^- conductance or if phosphorylation is involved.

Discussion

In the present study we have identified the ionic current used by squid ORNs to transduce the repellent odorant, betaine, into hyperpolarizing receptor potentials. Selectivity studies performed in voltage clamp showed that betaine activated a Cl^- selective current that was reversibly blocked by the Cl^- channel blockers SITS and niflumic acid. The odor responses were dose dependent with an EC_{50} for betaine of 4.4 mmol · l^{-1}. The lack of increase in $[Ca^{2+}]_i$ associated with odor application, suggests that Ca^{2+} is not involved, and that the Cl^- channel is not Ca^{2+} dependent. Gramicidin-patch experiments revealed that the normal $[Cl^-]_i$ is low (~50 mmol · l^{-1} compared to 440 mmol · l^{-1} external Cl^-) indicating that betaine would hyperpolarize tonically active ORNs and inhibit the firing of action potentials in vivo.

Hyperpolarization of ORNs

Hyperpolarization of ORNs can be accomplished by four mechanisms: 1) activating K^+ channels, 2) closing non-selective cation channels, 3) closing Cl^- channels if E_{Cl} is positive to E_{Rest}, and 4) activating Cl^- channels if E_{Cl} is negative to E_{Rest}. ORNs from various species have been identified that utilize one or more of the first three mechanisms. Examples of mechanism 1, include the moth (Stengl et al. 1992) and toad (Morales et al. 1994; Morales et al. 1995; Morales et al. 1997), where Ca^{2+}-activated K^+ channels mediate hyperpolarizations. In lobster, a cAMP-dependent K^+ channel underlies hyperpolarizing responses to odors (Michel and Ache 1992, 1994). Mechanism 2 has been observed in the moth *Antheraea polyphemus* (Zufall et al. 1991) and in the fly *Drosophila melanogaster* (Dubin and Harris 1997) where decreases in non-selective cation conductances hyperpolarize the cell. Mechanism 3, involving a decrease in the resting Cl^- conductance, has been observed

in *Drosophila* (Dubin and Harris 1997) and in mudpuppy (Dubin and Dionne 1994) ORNs. However, our work represents the first example of mechanism 4, which involves activating Cl^- channels when E_{Cl} is negative to the threshold for spiking. In most ORNs, $[Cl^-]_i$ is relatively high and E_{Cl} is usually less negative than E_{Rest} (Kurahashi and Yau 1993; Dubin and Dionne 1994; Zhainazarov and Ache 1995) so that activation of a Cl^- conductance will generate a depolarizing receptor potential. Using the GP technique on squid ORNs, we found that E_{Cl} could be as negative as −67 mV and averaged −57 mV, which would result in a hyperpolarizing receptor potential.

What are the implications of odorants that hyperpolarize ORNs? Given that squid ORNs often show basal activity (our unpublished observations), the hyperpolarization itself could be an important signal (Michel and Ache 1994). Because odors are usually present in mixtures, hyperpolarization could suppress tonic activity in sensory neurons that lack receptors for the excitatory odorant. This inhibition would increase the signal-to-noise ratio similar to inhibitory feedback networks in other systems. In addition, a hyperpolarization leading to a decrease in tonic firing, could disinhibit a higher pathway, as is found in mammalian ventral tegmental neurons (Johnson and North 1992). Finally, if ORNs contain more than one receptor type, odors that activate the hyperpolarizing conductance could reset the sensitivity of the neuron to excitatory odors (Michel and Ache 1994). Our future studies with excitatory odorants will specifically address the latter possibility.

Transduction pathways in squid ORNs

Various classes of Cl^- channels can be activated by voltage, neurotransmitters, Ca^{2+}, and cAMP (Delay et al. 1997). Although the specific pathway for activating the betaine-induced Cl^- current has yet to be identified, our studies to date make a number of potential mechanisms unlikely. The Cl^- currents in this study were not voltage dependent and were not active in the absence of ligand (betaine). Internal Ca^{2+} did not change with betaine application and phospholipase C inhibitors did not block betaine responses. Arachidonic acid did not activate a Cl^- current, and cAMP activated a cationic current (Lucero and Piper 1994). In addition, the lack of an inward current in the presence of Cl^- channel blockers supports the idea that cations do not enter from the outside. Finally, we eliminated the possibility that betaine was activating some type of a cation-dependent pump or transporter by recording betaine responses in the absence of internal and external Na^+ and K^+. Although we have ruled out the obvious second messengers in betaine responses, further experiments will be necessary to determine the mechanism underlying the betaine-activated Cl^- current. Possible mechanisms include Na^+- or K^+-independent pumps or transporters, a betaine-gated Cl^- channel, similar to other ligand-activated Cl^- channels such as the $GABA_A$ and glycine receptors, or a phosphorylation-dependent Cl^- channel.

Dose dependence of betaine

Betaine responses were dose dependent and show that betaine has a relatively high EC_{50} of 4.4 $mmol \cdot l^{-1}$. Betaine is widely used as an osmoregulator in marine organisms, and very high concentrations are found in the blood (4 $mmol \cdot l^{-1}$) and axoplasm (74 $mmol \cdot l^{-1}$) of the squid, *Loligo* (Deffner 1961). One hypothesis for the high EC_{50} of betaine is that since squid are shoaling animals (Hanlon and Messenger 1996), it is possible that low levels of betaine would be continuously present in their normal environment, and only millimolar concentrations, which might be released during predation attacks, would be of any significance to the animal. Behavioral experiments have shown that betaine is an aversive odorant to live squid at a concentration of 100 $\mu mol \cdot l^{-1}$ (Lee et al. 1994). While this is over an order of magnitude lower than the EC_{50} for dissociated cells, we have recorded responses from isolated ORNs to betaine concentrations as low as 1 $\mu mol \cdot l^{-1}$ (Fig. 7B). Furthermore, since such a large percentage of cells respond to betaine (60%), the concentration needed to behaviorally stimulate the animal may be much lower than the concentration needed to stimulate the isolated cells, due to summation of responses from hundreds of individual cells.

Physiological role of chloride in ORNs

The discovery of a novel, hyperpolarizing Cl^- conductance in squid ORNs adds another element to the debate on the role of Cl^- in olfactory signal transduction. It has been suggested that, in mammals, Ca^{2+}-activated Cl^- currents result in a non-linear amplification of odor responses (Lowe and Gold 1993). This model of amplification assumes that E_{Cl} is much less negative than E_{Rest}, and that activating a Cl^- conductance will depolarize the cell. The natural E_{Cl} of ORNs from different species cannot be assumed. In amphibians, where it has been carefully measured in frog (Zhainazarov and Ache 1995), mudpuppy (Dubin and Dionne 1994), and newt (Nakamura et al. 1997), E_{Cl} ranges from −45 to 0 mV, suggesting that E_{Cl} can be quite variable, even within a single phylogenetic class. Although we cannot exclude a compartmentalization of chloride concentrations which might alter E_{Cl} at the sight of transduction (Firestein and Shepherd 1995), our data from squid show that E_{Cl} can be even more negative than in Amphibia. Clearly, Cl^- plays an important role in olfactory transduction, but its specific effects cannot be assigned without determining E_{Cl}.

Acknowledgements We would like to thank Drs. Peter Barry and Mike Michel for reading the manuscript and providing useful

comments. We also thank Jimmy Lucero and David Piper for technical support. This work was supported by ONR #N00014-89-J-1744 and NIH NIDCD #DC 02587-02 to MTL.

These experiments comply with NIH publication No. 86–23, "Principles of animal care," revised 1985, and with the current laws of the United States regarding animal research.

References

Abe Y, Furukawa K, Itoyama Y, Akaike N (1994) Glycine response in acutely dissociated ventromedial hypothalamic neuron of the rat: new approach with gramicidin perforated patch-clamp technique. J Neurophysiol 72: 1530–1537

Ache BW, Zhainazarov A (1995) Dual second-messenger pathways in olfactory transduction. Curr Opin Neurobiol 5: 461–466

Boekhoff I, Raming K, Breer H (1990a) Pheromone-induced stimulation of inositol-trisphosphate formation in insect antennae is mediated by G-proteins. J Comp Physiol B 160: 99–103

Boekhoff I, Tareilus E, Strotmann J, Breer H (1990b) Rapid activation of alternative second messenger pathways in olfactory cilia from rats by different odorants. EMBO J 9: 2453–2458

Breer H, Boekhoff I, Tareilus E (1990) Rapid kinetics of second messenger formation in olfactory transduction. Nature (Lond) 345: 65–68

Bruch RC, Teeter JH (1989) Second messenger signalling mechanisms in olfaction. In: Brand JG, Teeter JH, Kare MR, Cagan RH (eds) Receptor and transduction mechanisms in taste and olfaction. Dekker, New York

Buck L, Axel R (1991) A novel multigene family may encode odorant receptors: a molecular basis for odor recognition. Cell 65: 175–187

Deffner GGJ (1961) The dialyzable free organic constituents of squid blood: a comparison with nerve axoplasm. Biochim Biophys Acta 47: 378–388

Delay RJ, Dubin AE, Dionne VE (1997) A cyclic-nucleotide-dependent chloride conductance in olfactory receptor neurons. J Membr Biol 159(1): 53–60

Dionne VE, Dubin AE (1994) Transduction diversity in olfaction. J Exp Biol 194: 1–21

Dubin AE, Dionne VE (1994) Action potentials and chemosensitive conductances in the dendrites of olfactory neurons suggest new features for odor transduction. J Gen Physiol 103: 181–201

Dubin AE, Harris GL (1997) Voltage-activated and odor-modulated conductances in olfactory neurons of *Drosophila melanogaster*. J Neurobiol 32: 123–137

Fadool DA, Ache BW (1992) Plasma membrane inositol 1,4,5-trisphosphate-activated channels mediate signal transduction in lobster olfactory receptor neurons. Neuron 9: 907–918

Firestein S, Shepherd GM (1995) Interaction of anionic and cationic currents leads to a voltage dependence in the odor response of olfactory receptor neurons. J Neurophysiol 73: 562–567

Firestein S, Zufall F, Shepherd GM (1991) Single odor-sensitive channels in olfactory receptor neurons are also gated by cyclic nucleotides. J Neurosci 11: 3565–3572

Gesteland RC, Lettvin JY, Pitts WH (1965) Chemical transmission in the nose of the frog. J Physiol (Lond) 181: 525–559

Gilly WF, Lucero MT (1992) Behavioral responses to chemical stimulation of the olfactory organ in the squid *Loligo opalescens*. J Exp Biol 162: 209–229

Gold GH, Nakamura T (1987) Cyclic nucleotide-gated conductances: a new class of ion channels mediates visual and olfactory transduction. TIPS 8: 312–316

Grynkiewicz G, Poenie M, Tsien RY (1985) A new generation of Ca^{+2} indicators with greatly improved fluorescence properties. J Biol Chem 260: 3440–3450

Hanlon RT, Messenger JB (1996) Cephalopod behavior. Cambridge University Press, Cambridge, pp 149–171

Hille B (1992) Ionic channels of excitable membranes. Sinauer, Sunderland, MA

Horn R, Marty A (1988) Muscarinic activation of ionic currents measured by a new whole-cell recording method. J Gen Physiol 92: 145–159

Johnson SW, North RA (1992) Two types of neurone in the rat ventral tegmental area and their synaptic inputs. J Physiol (Lond) 450: 455–468

Kang J, Caprio J (1995) In vivo responses of single olfactory receptor neurons in the channel catfish, *Ictalurus punctatus*. J Neurophysiol 73: 172–177

Kashiwayanagi M, Kawahara H, Kanaki K, Nagasawa F, Kurihara K (1996) Ca^{2+} and Cl^{-}-dependence of the turtle olfactory response to odorants and forskolin. Comp Biochem Physiol A 115A: 43–52

Kleene SJ (1993) Origin of the chloride current in olfactory transduction. Neuron 11: 123–132

Kleene SJ, Gesteland RC (1991) Calcium-activated chloride conductance in frog olfactory cilia. J Neurosci 11: 3624–3629

Kurahashi T, Yau K-W (1993) Co-existence of cationic and chloride components in odorant-induced current of vertebrate olfactory receptor cells. Nature (Lond) 363: 71–74

Lee PG (1992) Chemotaxis by *Octopus maya* Voss et Solis in a Y-maze (abstract) J Exp Biol Ecol 153: 53–67

Lee PG, DiMarco FP, Hanlon RT (1994) Chemoreception and feeding behavior in cephalopods (abstract). Equense, Italy

Lo YH, Bradley TM, Rhoads DE (1993) Simulation of Ca^{2+}-regulated olfactory phospholipase C by amino acids. Biochemistry 32: 12358–12362

Lowe G, Gold GH (1993) Nonlinear amplification by calcium-dependent chloride channels in olfactory receptor cells. Nature (Lond) 366: 283–286

Lucero MT, Chen NS (1997) Characterization of voltage- and Ca^{2+}-activated K^{+} channels in squid olfactory receptor neurons. J Exp Biol 200: 1571–1586

Lucero MT, Piper DR (1994) IP3 and cyclic nucleotides elicit opposite membrane potential changes in squid olfactory receptor neurons (abstract). Chem Senses 19: 509

Lucero MT, Horrigan FT, Gilly WF (1992) Electrical responses to chemical stimulation of squid olfactory receptor cells. J Exp Biol 162: 231–249

Lucero MT, Piper DR, Gilly WF (1995) Dopamine increases internal Ca^{+2} in squid olfactory receptor neurons (abstract). Chem Senses 19: 509

Marty A, Neher E (1995) Tight-seal whole-cell recording. In: Sakmann B, Neher E (eds) Single-channel recording. Plenum, New York, pp 31–51

McClintock TS, Ache BW (1989) Hyperpolarizing receptor potentials in lobster olfactory receptor cells: implications for transduction and mixture suppression. Chem Senses 14: 637–647

Michel WC, Ache BW (1992) Cyclic nucleotides mediate an odor-evoked potassium conductance in lobster olfactory receptor cells. J Neurosci 12: 3979–3984

Michel WC, Ache BW (1994) Odor-evoked inhibition in primary olfactory receptor neurons. Chem Senses 19: 11–24

Miyamoto T, Restrepo D, Cragoe EJJ, Teeter JH (1992) IP_3 and cAMP-induced responses in isolated olfactory receptor neurons from the channel catfish. J Membr Biol 127: 173–183

Morales B, Ugarte G, Labarca P, Bacigalupo J (1994) Inhibitory K^{+} current activated by odorants in toad olfactory neurons. Proc R Soc Lond Ser B 257: 235–242

Morales B, Labarca P, Bacigalupo J (1995) A ciliary K^{+} conductance sensitive to charibdotoxin underlies inhibitory responses in toad olfactory receptor neurons. FEBS Lett 359: 41–44

Morales B, Madrid R, Bacigalupo J (1997) Calcium mediates the activation of the inhibitory current induced by odorants in toad olfactory receptor neurons. FEBS Letters 402: 259–264

Myers VB, Hayden DA (1972) Ion transfer across lipid membranes in the presence of gamicidin A. II. The ion selectivity. Biochim Biophys Acta 274: 313–322

Nakamura T, Nishida N, Kaneko H (1997) Direct measurement of concentration of chloride in the newt olfactory cell (abstract). Chem Senses 22: 757–758

Restrepo D, Boekhoff I, Breer H (1993) Rapid kinetic measurements of second messenger formation in olfactory cilia from channel catfish. Am J Physiol Cell Physiol 264: C906–C911

Restrepo D, Teeter JH, Schild D (1996) Second messenger signaling in olfactory transduction. J Neurobiol 30: 37–48

Robinson RA, Stokes RH (1968) Electrolyte solutions: the measurement and interpretation of conductance, chemical potential and diffusion in solutions of simple electrolytes. Butterworths, London

Ronnett GV, Cho H, Hester LD, Wood SF, Snyder SH (1993) Odorants differentially enhance phosphoinositide turnover and adenylyl cyclase in olfactory receptor neuronal cultures. J Neurosci 13: 1751–1758

Stengl M, Zufall F, Hatt H, Hildebrand JG (1992) Olfactory receptor neurons from antennae of developing male *Manduca sexta* respond to components of the species-specific sex pheromone in vitro. J Neurosci 12: 2523–2531

Woodbury JW, Miles PR (1973) Anion conductance of frog muscle membranes: one channel, two kinds of pH dependence. J Gen Physiol 62: 324–353

Zhainazarov AB, Ache BW (1995) Odor-induced currents in *Xenopus* olfactory receptor cells measured with perforated-patch recording. J Neurophysiol 74: 479–483

Zufall F, Hatt H, Keil TA (1991) A calcium-activated nonspecific cation channel from olfactory receptor neurones of the silkmoth *Antheraea polyphemus*. J Exp Biol 161: 455–468

Zufall F, Firestein S, Shepherd GM (1994) Cyclic nucleotide-gated ion channels and sensory transduction in olfactory receptor neurons. Annu Rev Biophys Biomol Struct 23: 577–607